with the O···O interactions in (I) and (II), then since the C(H)···methyl interactions are also similar, we must come to the conclusion that the energy required to further deform the phenanthrene and naphthalene cores is also similar. This, however, appears unlikely since the phenanthrene nucleus is grossly distorted yet the naphthalene nucleus is not significantly distorted. If we consider the energy profiles for deformation of these molecules as parabolas then in the phenanthrene case the observed structure would lie some way up the steep side of the curve and in the naphthalene case the structure lies close to the valley of the curve. Given that the O···O interaction in the naphthalene case is highly unfavourable then we would expect to see some distortion of the nucleus. Thus, we conclude that comparison of the present two structures indicates that it is easier to bring atoms close together side on, as in naphthalene, than more nearly head on, as in phenanthrene, unless the naphthalene nucleus is extraordinarily difficult to deform in the direction perpendicular to the aromatic rings.

References

Bondi, A. (1964). *J. Chem. Phys.* **68**, 441–451.
Bott, G., Field, L. D. & Sternhell, S. (1980). *J. Am. Chem. Soc.* **102**, 5618–5626.
Buu-Hoi, N. P. & Lavit, D. (1956). *J. Chem. Soc.* pp. 2412–1415.
Cosmo, R., Hambley, T. W. & Sternhell, S. (1987*a*). *J. Org. Chem.* **52**, 3119–3123.
Cosmo, R., Hambley, T. W. & Sternhell, S. (1987*b*). *Tetrahedron Lett.* **28**, 6239–6240.
Cosmo, R. & Sternhell, S. (1987*a*). *Aust. J. Chem.* **40**, 35–47.
Cosmo, R. & Sternhell, S. (1987*b*). *Aust J. Chem.* **40**, 2137–2142.
Germain, G., Main, P. & Woolfson, M. M. (1971). *Acta Cryst.* A**27**, 368–379.
Guss, J. M. (1976). *SUSCAD*. Data reduction for the CAD-4 diffractometer. Univ. of Sydney, Australia.
International Tables for X-ray Crystallography (1974). Vol. IV. Birmingham: Kynoch Press. (Present distributor Kluwer Academic Publishers, Dordrecht.)
Johnson, C. K. (1965). *ORTEP*. Report ORNL-3794. Oak Ridge National Laboratory, Tennessee, USA.
Kay, M. I., Okaya, Y. & Cox, D. E. (1971). *Acta Cryst.* B**27**, 26–33.
Sheldrick, G. M. (1976). *SHELX76*. Program for crystal structure determination. Univ. of Cambridge, England.
Sternhell, S. & Tansey, C. W. (1987). Unpublished results.
Trotter, J. (1963). *Acta Cryst.* **16**, 605–608.

Acta Cryst. (1990). B**46**, 562–567

Structure of Belladonna Mottle Virus: Cross-Rotation Function Studies with Southern Bean Mosaic Virus

By C. N. Hiremath, S. K. Munshi and M. R. N. Murthy

Molecular Biophysics Unit, Indian Institute of Science, Bangalore 560 012, *India*

(*Received* 15 *November* 1989; *accepted* 26 *February* 1990)

Abstract

Belladonna mottle virus, which belongs to the tymovirus group of RNA plant viruses, crystallizes in rhombohedral space group $R3$ with $a = 295{\cdot}38$ Å and $\alpha = 59{\cdot}86°$. Cross-rotation function studies between belladonna mottle virus and southern bean mosaic virus reveal that the structure of this tymovirus is similar to those of sobemo viruses. A procedure for computing an icosahedrally averaged rotation function was developed as a general method for a more precise determination of the orientation of a symmetric molecule in an unknown cell. These studies suggest that it might be possible to obtain a high-resolution structure of belladonna mottle virus starting from phases derived from a model based on southern bean mosaic virus.

1. Introduction

Belladonna mottle virus (BDMV; Moline & Fries, 1974) belongs to the tymovirus group of monopartite RNA plant viruses. The type member of this group, turnip yellow mosaic virus (TYMV) has been extensively studied in terms of the forces stabilizing the particle structure (Kaper, 1971, 1975; Jacrot, Chauvin & Witz, 1977; Katouzian-Safadi, Favre & Haenni, 1980; Katouzian-Safadi & Berthet-Colominas, 1983; Katouzian-Safadi & Haenni, 1986; Keeling & Matthews, 1982). The integrity of the particle structure in these viruses is derived from strong hydrophobic association of protein subunits. Electron micrographs of TYMV particles prepared by the negative staining technique show 32 morphological units in an icosahedral arrangement (Nixon & Gibbs, 1960; Mellema & Amos, 1972). Neutron scattering experiments have revealed that there is little penetration of nucleic acid into the densely packed protein coat of TYMV (Jacrot *et al.*, 1977).

The amino-acid sequence of the coat proteins of three tymoviruses, TYMV (Peter, Stehelin, Reinbolt, Collot & Duranton, 1972), eggplant mosaic virus

0108-7681/90/040562-06$03.00

(EMV; Dupin, Peter, Collot, Das, Peter, Bouillon & Duranton, 1984) and BDMV (Suryanarayana, Appaji Rao, Murthy & Savithri, 1989), have been determined. These sequences share extensive regions of homology suggesting that their secondary and tertiary structures are similar. In contrast to several other spherical plant viruses, tymoviruses lack a basic amino terminal segment in their coat protein (Suryanarayana, Jacob & Savithri, 1988). Such basic amino termini partially neutralize the negative charges of RNA phosphates and appear to play an important role in the nucleocapsid assembly of several viruses (Savithri & Erickson, 1983; Chidlow & Tremaine, 1971; Cuillel, Jacrot & Zulauf, 1981; Bol, Kraal & Brederode, 1974). Lack of a basic amino terminal segment is compensated for by polyamines and calcium which are bound as intrinsic components of BDMV, EMV and TYMV (Savithri, Munshi, Suryanarayana, Divakar & Murthy, 1987; Durham, Witz & Bancroft, 1984; Cohen & Greenberg, 1981). In BDMV, replacement of polyamines by monovalent ions results in the instability of virus particles at alkaline pH (Savithri *et al.*, 1987).

X-ray crystallographic studies on tymoviruses have been initiated in several laboratories. TYMV was one of the earliest viral crystalline preparations to be examined by X-ray methods (Bernal & Carlisle, 1948). Even before the advent of modern structural methods, Klug, Longley & Lebermann (1966) subjected single crystals of TYMV to X-ray diffraction studies and concluded that the observed transforms are consistent with icosahedral symmetry. Crystallization and preliminary characterization of the rhombohedral crystals of BDMV was reported by Heuss, Mohana Rao & Argos (1981). Colman, Tulloch, Shukla & Gough (1980) deduced the particle and crystal symmetry of erysimum latent virus by electron micrography and X-ray analysis of single crystals. We have earlier reported rotation function calculations establishing the icosahedral symmetry of virus particles based on a partial set of 5·5 Å data for the rhombohedral crystals of BDMV (Munshi, Hiremath, Murthy & Savithri, 1987). Cross-rotation function studies with X-ray diffraction data from crystals of SBMV (Abad-Zapatero, Abdel-Mequid, Johnson, Leslie, Rayment, Rossmann, Suck & Tsukihara, 1980) suggested the possibility of structure determination starting from an initial model based on the SBMV particle structure.

2. Materials and methods

BDMV was purified and crystallized as described elsewhere (Savithri *et al.*, 1987; Munshi *et al.*, 1987). The crystals are rhombohedral, space group $R3$, with $a = 295{\cdot}38$ Å and $\alpha = 59{\cdot}85°$, and isomorphous to those reported by Heuss *et al.* (1981). The unit cell contains one virus particle with its icosahedral threefold axis coincident with the crystal threefold axis. X-ray diffraction data were collected by screenless oscillation photography using crystals mounted with their threefold axis coincident with the camera spindle axis. A total of 70 A/B film pairs were recorded covering a crystal rotation of 50°. For rhombohedral $R3$ crystals, a rotation of 45° about the threefold axis is sufficient to record a complete asymmetric unit of reciprocal space (Munshi & Murthy, 1986). The other details of data collection and processing were similar to those reported for the rotation function studies (Munshi *et al.*, 1987). Details of the data collected are presented in Table 1.

Table 1. *Oscillation-data collection*

	Native crystals
Oscillation range	1°
Crystal-to-film distance	100 mm
Overlaps of neighbouring oscillation ranges	0·2°
Resolution for processing	5·5 Å
Approximate exposure time	20 h
Number of A/B pairs	70
Number of measurements	68 326
Independent reflections	43 363
R factor*	10·3%
Rejection criteria on F^2	2σ
Cell dimensions and mosaicity after post-refinement†	$a = 295{\cdot}38$ Å $\alpha = 59{\cdot}86°$ $m = 0{\cdot}08°$

* $R = [\sum_h \sum_i |(\langle I_h \rangle - I_{hi})| / \sum_h \sum_i I_{hi}] \times 100{\cdot}0$, where $\langle I_h \rangle$ is the mean of i observations (I_{hi}) of reflection h.

† For a definition of the mosaicity parameter, see Rossmann (1979).

3. Results and discussion

Rotation function studies

The three-dimensional structures of several spherical viruses determined in recent years are built from protein subunits characterized by eight-stranded β-barrel motifs of remarkably similar topology (Liljas, 1986). These similarities and the invariable redundancy of structural information present in the structures of icosahedral viruses offer the attractive possibility of faster structure determination through molecular-replacement techniques (Acharya, Fry, Stuart, Fox, Rowlands & Brown, 1989). The amino-acid sequence of BDMV coat protein is not homologous to those of other $T = 3$ icosahedral plant viruses of known three-dimensional structure. However, BDMV is closer to SBMV in terms of coat protein size and triangulation number. Cross-rotation function (Rossmann & Blow, 1962) studies were therefore carried out to assess the similarities that might exist between BDMV and SBMV and to explore the possibility of using the SBMV model for determining the structure of BDMV.

An orthogonal coordinate system (Fig. 1) with the *Y* axis aligned with the crystal threefold axis was used in our earlier studies on BDMV (Munshi *et al.*, 1987). This coordinate system is convenient for the interpretation of rotation functions. The published rotation functions of SBMV are expressed in an orthogonal system derived from the hexagonal setting of the rhombohedral lattice (Rayment, Johnson, Suck, Akimoto & Rossmann, 1978). In order to simplify interpretation of rotation function results, all the calculations were carried out in the Cartesian system defined for BDMV. An example of the recomputed self-rotation function for SBMV, using the data kindly supplied by Professor M. G. Rossman, and the corresponding function for BDMV are shown in Fig. 2. The self-rotation function peak positions were invariant with respect to parameters such as radius of integration, resolution limits and number of terms selected to represent the second Patterson function. The peaks in the self-rotation functions of SBMV are on mirror planes and hence are expected to be twice as significant as those of the BDMV rotation function, which are in general positions.

The position of the peak in the cross-rotation function if the two virus structures are similar is easily deduced from an inspection of the rotation functions depicted in Fig. 2. Thus, if the BDMV Patterson function is rotated while the threefold axes of the two Pattersons are aligned, a large peak at $K \simeq 38°$ is expected in the cross-rotation function. Fig. 3(*a*) depicts the cross-rotation function computed using the data between 11 and 13 Å resolution with other parameters identical to those used for the self-rotation functions. The anticipated peak at $k \simeq 38°$ is the major feature of this function. In order to check that the rotation function peak is not merely an artefact of the superposition of icosahedral axes, rotation functions were computed using only terms from shells of increasing resolution. The peak at $K \simeq 38°$ was the major feature of functions computed in ranges 15–50, 11–15, 8–11 and 5·5–8 Å. However, both the self-rotation function for BDMV and the cross-rotation function with SBMV, computed between 6 and 8 Å resolution, did not show significant peaks at the anticipated positions for some unknown reason.

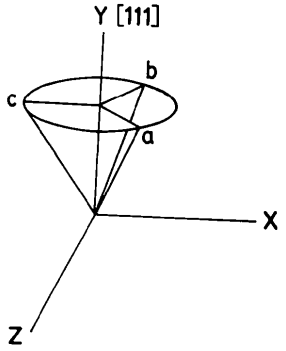

Fig. 1. Definition of the Cartesian coordinate system used for rotation function calculations. The crystal threefold axis (rhombohedral [111]) was defined as Cartesian *Y* axis, and the crystal *c* axis is in the *XY* plane with a negative projection on the *X* axis.

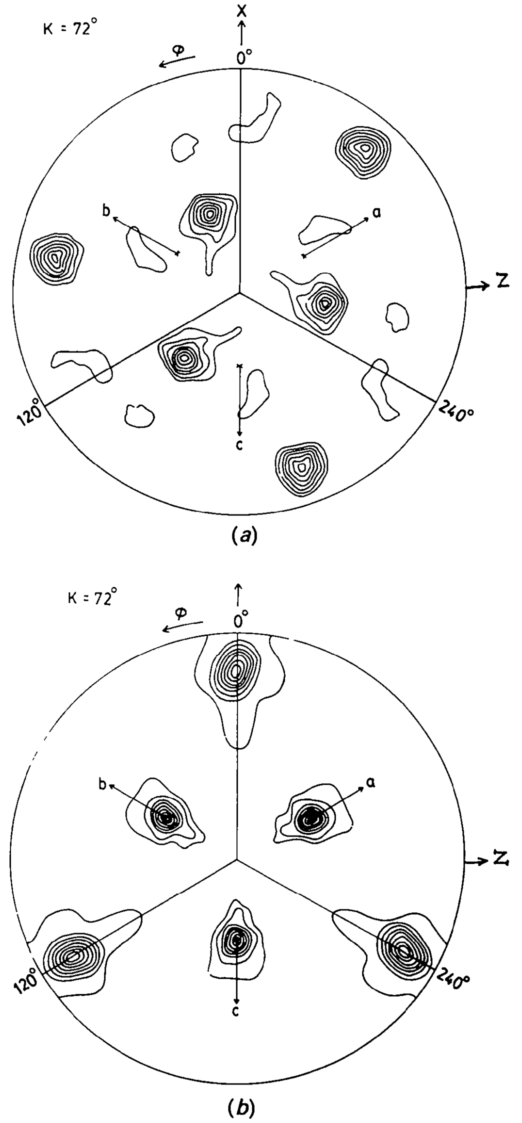

Fig. 2. Stereographic projections of the rotation functions of (*a*) BDMV and (*b*) SBMV corresponding to $K = 72°$. Both functions were computed using data between 11 and 13 Å with a radius of integration of 50 Å. The contours are drawn at 2σ intervals starting at 2σ above the mean background. The orientation of the crystallographic axes is also shown.

Icosahedrally averaged rotation function

There are 20 different orientations of the BDMV particle that are crystallographically independent but related by icosahedral symmetry. Superposition of the SBMV Patterson with any of the 20 equivalent orientations of the BDMV Patterson results in cross-rotation function values related by particle symmetry. Averaging the value of the function over these 20 icosahedrally related orientations is likely to increase the sensitivity of detecting structural similarities and provide a more accurate relationship between particle orientations in the respective unit cells. The derived function is called an icosahedrally averaged rotation function. A similar function has been used by Rossmann, Ford, Watson & Banaszak (1972) and Arnold, Vriend, Luo, Griffith, Kamer, Erickson, Johnson & Rossmann (1987). The averaged function is computed as follows:

$$R = \int P_1(x_1)P_2(x_2)\mathrm{d}x_1$$

$$x_2 = [c]x_1$$

and

$$[c] = [OTC]_2[\rho][CTO]_1.$$

$[CTO]_1$ is the crystal fractional to orthogonal Cartesian transformation for compound 1 (P_1), $[OTC]_2$ is the Cartesian to crystal fractional coordinate transformation matrix for compound 2 (P_2), and $[\rho]$ is an orthogonal rotation matrix. Let $[s]$ be the collection of matrices representing the symmetry of the virus particle in the orthogonal system. The fractional coordinate x_{1R} is related to x_1 by non-crystallographic symmetry,

$$x_{1R} = [CTO^{-1}]_1[s_i][CTO]_1x_1. \quad (1)$$

Hence, the rotation function for the non-crystallographically related orientation is

$$R' = \int P_1(x_{1R})P_2(x_2)\mathrm{d}x_{1R}. \quad (2)$$

The transformation between x_{1R} and x_2 is as follows:

$$x_2 = [OTC]_2[\rho][CTO]_1x_1$$

$$x_2 = [OTC]_2[\rho][s_i^{-1}][CTO]_1x_{1R},$$

where $[s_i^{-1}]$ corresponds to a non-crystallographic symmetry. Thus, for each set of Eulerian or polar angles, values of the function are evaluated using the 20 transformations:

$$[\rho_i] = [\rho][s_i^{-1}].$$

The average rotation function value ('sum function') or the mean of a few of the smallest R values ('minimum function') can be plotted as a function of the variables chosen for the representation of the function. Such an icosahedrally averaged function is likely to have a better signal-to-noise ratio and minimal variation in the background, with a few, if any, spurious features (Fig. 3*b*). The peak at $K = 38°$ in the unaveraged function (Fig. 3*a*) is at about the 4σ level, while that of the averaged function (Fig. 3*b*) is at 7σ. The peak at $K \simeq 100°$, which is probably due to the quasi-sixfold character of the icosahedral threefold axis at this resolution, is significantly reduced in the averaged function.

Icosahedrally averaged cross-rotation functions computed using the 15–50, 11–15, 8–11 and 5·5–8 Å data shells are shown in Fig. 4. The peak corresponding to $K = 38°$ is present in all the functions. As anticipated, the functions at higher resolution are sharper and allow more precise determination of the structural relationship. These results imply that the Patterson functions of the two compounds can be

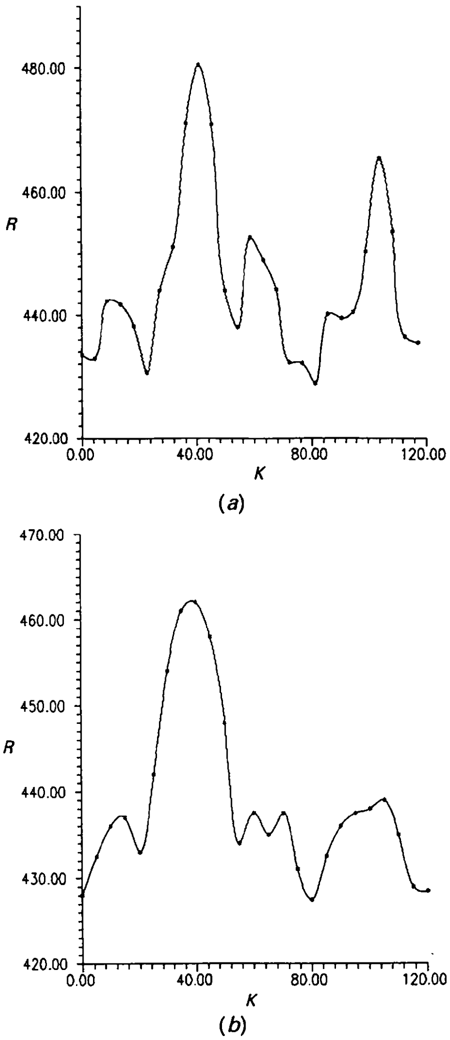

Fig. 3. Cross-rotation function between BDMV (compound 1) and SBMV (compound 2) as a function of rotation K about the superimposed threefold axis. The resolution limits and the radius of integration used are identical to those of Fig. 2. (*a*) Function corresponding to one of the 20 transformations related by molecular symmetry. (*b*) 20-Fold averaged function.

made to overlap by a rotation which results in precise superposition of the icosahedral symmetry axes of the two virus particles. The matrix that transforms the *PQR* coordinates of SBMV subunits deposited in the Protein Data Bank (Bernstein, Koetzle, Williams, Meyer, Brice, Rogers, Kennard, Shimanouchi & Tasumi, 1977) to the orthogonal system used in these studies is

$$[T]=\begin{bmatrix} -0{\cdot}1419 & 0{\cdot}9884 & 0{\cdot}0543 \\ 0{\cdot}3568 & 0{\cdot}0000 & 0{\cdot}9342 \\ 0{\cdot}9233 & 0{\cdot}1520 & -0{\cdot}3527 \end{bmatrix}.$$

Concluding remarks

Cross-rotation function studies between BDMV and SBMV clearly demonstrate that the tertiary and quaternary structures of tymoviruses closely resemble those of sobemo viruses. The procedure for computing the icosahedrally averaged rotation function described here might be used as a general method for a more precise determination of the orientation of a molecule in an unknown crystal cell for biological macromolecules with a high degree of internal symmetry. Evidence for the structural similarities between tymoviruses and sobemo viruses was obtained using this procedure. Studies carried out at increasingly higher resolution shells suggest that the structure of BDMV might be determined starting from phases based on an SBMV model, followed by phase refinement by molecular-replacement techniques exploiting the 20-fold redundancy of structural information in the asymmetric unit of the BDMV crystal.

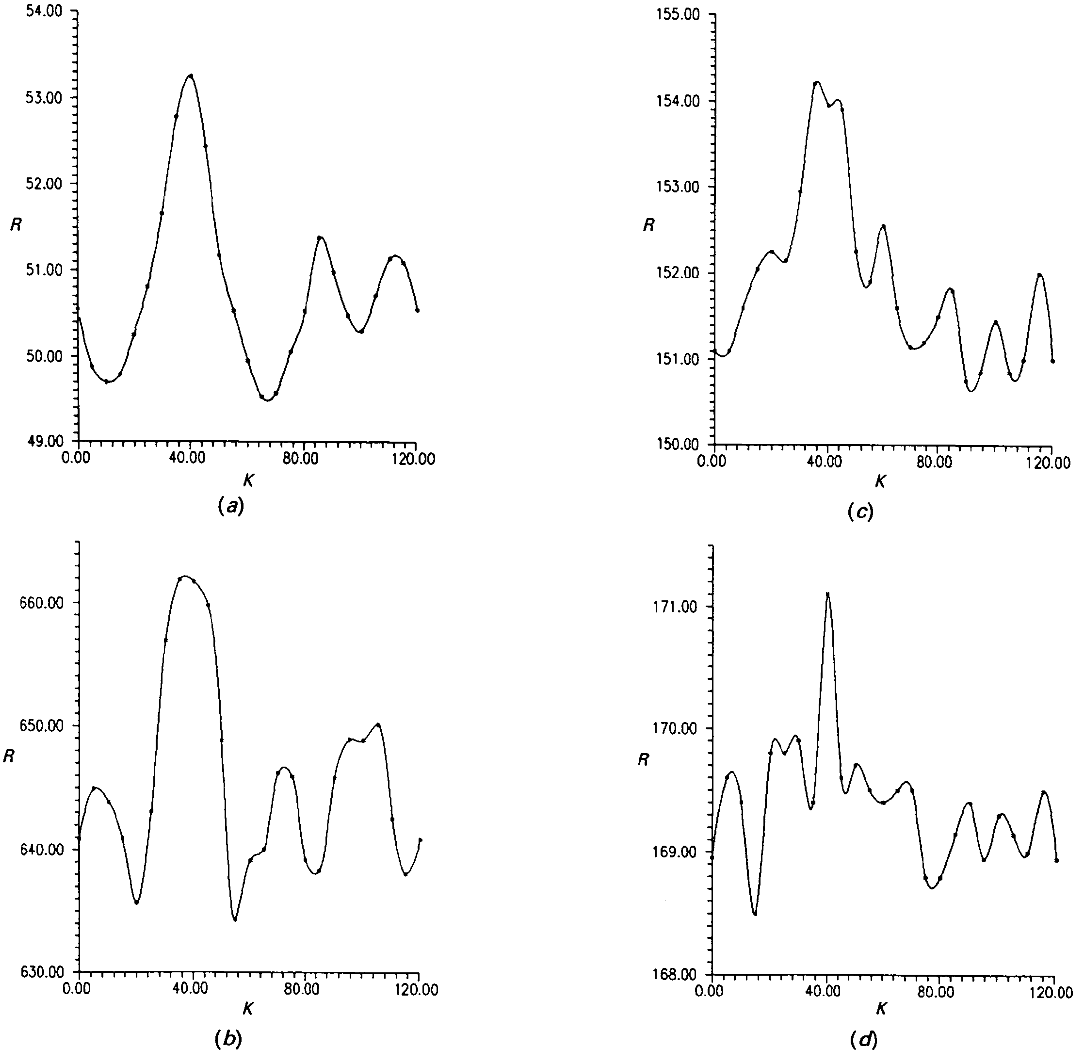

Fig. 4. Icosahedrally averaged cross-rotation function between BDMV and SBMV as a function of rotation *K* about the superimposed threefold axis. The radius of integration was 50 Å and terms greater than 2·5 times the average intensity were chosen to represent the second Patterson. (*a*) 15–50 Å, (*b*) 11–15 Å, (*c*) 8–11 Å and (*d*) 5·5–8 Å.

We thank M. G. Rossmann, Purdue University, for providing SBMV data, and I. Rayment, Arizona University, and M. G. Rossmann for providing some programs. T. U. Sahana and G. Govindswamy provided excellent technical assistance. This work was supported by the Department of Science and Technology, India.

References

Abad-Zapatero, C., Abdel-Mequid, S. S., Johnson, J. E., Leslie, A. G. W., Rayment, I., Rossmann, M. G., Suck, D. & Tsukihara, T. (1980). *Nature* (*London*), **286**, 33–39.

Acharya, R., Fry, E., Stuart, D., Fox, G., Rowlands, D. & Brown, F. (1989). *Nature* (*London*), **337**, 709–716.

Arnond, E., Vriend, G., Luo, M., Griffith, J. P., Kamer, G., Erickson, J. W., Johnson, J. E. & Rossmann, M. G. (1987). *Acta Cryst.* A**43**, 346–361.

Bernal, J. D. & Carlisle, C. H. (1948). *Nature* (*London*), **162**, 139–140.

Bernstein, F. C., Koetzle, T. F., Williams, G. J. B., Meyer, E. F., Brice, M. D., Rogers, J. R., Kennard, O., Shimanouchi, T. & Tasumi, M. J. (1977). *J. Mol. Biol.* **112**, 535–542.

Bol, J. F., Kraal, B. & Brederode, F. Th. (1974). *Virology*, **58**, 101–110.

Chidlow, J. & Tremaine, J. H. (1971). *Virology*, **43**, 267–278.

Cohen, S. S. & Greenberg, M. L. (1981). *Proc. Natl Acad. Sci. USA*, **78**, 5470–5474.

Colman, P. M., Tulloch, P. A., Shukla, D. D. & Gough, K. H. (1980). *J. Mol. Biol.* **142**, 263–268.

Cuillel, M., Jacrot, M. & Zulauf, M. (1981). *Virology*, **110**, 63–72.

Dupin, A., Peter, R., Collot, D., Das, B. C., Peter, C., Bouillon, P. & Duranton, H. (1984). *C. R. Acad. Sci. Sér. C*, **298**, 219–221.

Durham, A. C. H., Witz, J. & Bancroft, J. B. (1984). *Virology*, **133**, 1–8.

Heuss, K. L., Mohana Rao, J. K. & Argos, P. (1981). *J. Mol. Biol.* **146**, 629–633.

Jacrot, B., Chauvin, C. & Witz, B. (1977). *Nature* (*London*), **266**, 417–421.

Kaper, J. M. (1971). *J. Mol. Biol.* **56**, 259–276.

Kaper, J. M. (1975). *Frontiers of Biology*, Vol. 39, edited by A. Neuberger & E. L. Tatiem, pp. 273–320. Amsterdam: North-Holland.

Katouzian-Safadi, M. & Berthet-Colominas, C. (1983). *Eur. J. Biochem.* **137**, 47–55.

Katouzian-Safadi, M., Favre, A. & Haenni, A.-L. (1980). *Eur. J. Biochem.* **112**, 478–486.

Katouzian-Safadi, M. & Haenni, A.-L. (1986). *J. Gen. Virol.* **67**, 557–565.

Keeling, J. & Matthews, R. E. F. (1982). *Virology*, **119**, 214–218.

Klug, A., Longley, W. & Lebermann, R. (1966). *J. Mol. Biol.* **15**, 315–343.

Liljas, L. (1986). *Prog. Biophys. Mol. Biol.* **48**, 1–36.

Mellema, J. E. & Amos, L. A. (1972). *J. Mol. Biol.* **72**, 819–822.

Moline, H. E. & Fries, R. E. (1974). *Phytopathology*, **64**, 44–48.

Munshi, S. K., Hiremath, C. N., Murthy, M. R. N. & Savithri, H. S. (1987). *Acta Cryst.* B**43**, 376–382.

Munshi, S. K. & Murthy, M. R. N. (1986). *J. Appl. Cryst.* **19**, 61–62.

Nixon, H. L. & Gibbs, A. J., (1960). *J. Mol. Biol.* **2**, 197–200.

Peter, R., Stehelin, D., Reinbolt, J., Collot, D. & Duranton, H. (1972). *Virology*, **49**, 615–617.

Rayment, I., Johnson, J. E., Suck, D., Akimoto, T. & Rossmann, M. G. (1978). *Acta Cryst.* B**34**, 567–578.

Rossmann, M. G. (1979). *J. Appl. Cryst.* **12**, 225–238.

Rossmann, M. G. & Blow, D. M. (1962). *Acta Cryst.* **15**, 24–31.

Rossmann, M. G., Ford, G. C., Watson, H. C. & Banaszak, L. J. (1972). *J. Mol. Biol.* **64**, 237–249.

Savithri, H. S. & Erickson, J. W. (1983). *Virology*, **126**, 328–335.

Savithri, H. S., Munshi, S. K., Suryanarayana, S., Divakar, S. & Murthy, M. R. N. (1987). *J. Gen. Virol.* **68**, 1533–1542.

Suryanarayana, S., Appaji Rao, N., Murthy, M. R. N. & Savithri, H. S. (1989). *J. Biol. Chem.* **264**, 6273–6279.

Suryanarayana, S., Jacob, A. N. K. & Savithri, H. S. (1988). *Indian J. Biochem. Biophys.* **25**, 580–584.

Acta Cryst. (1990). B**46**, 567–572

Structure of 1,2-Dinitrobenzene

By Frank H. Herbstein and Moshe Kapon

Department of Chemistry, Technion–Israel Institute of Technology, Haifa, Israel 32000

(*Received* 2 *December* 1989; *accepted* 7 *March* 1990)

Abstract

$C_6H_4N_2O_4$, $M_r = 168{\cdot}11$, monoclinic, $P2_1/c$, $a = 7{\cdot}945\,(5)$, $b = 12{\cdot}975\,(8)$, $c = 7{\cdot}421\,(5)$ Å, $\beta = 111{\cdot}88\,(1)^\circ$, $V = 709{\cdot}90$ Å^3, $Z = 4$, D_m (flotation at 290 K) $= 1{\cdot}565$, $D_x = 1{\cdot}573$ g cm^{-3}, λ(Mo $K\alpha$) $= 0{\cdot}71069$ Å, μ(Mo $K\alpha$) $= 0{\cdot}90$ cm^{-1}, $F(000) = 344$, room temperature, $R_F = 0{\cdot}0541$ for 1444 observed reflections. The molecules are stacked along [001], with approximate hexagonal close packing of the stacks. The two nitro groups are twisted out of the mean plane of the benzene ring by angles of $\sim 41^\circ$, the molecule having very nearly $C_2 - 2$ symmetry. The anisotropic displacements of the atoms have been analysed in terms of the translational, librational and screw motions of the molecule as a unit, with the addition of internal torsional oscillations of the nitro groups about the C—N bonds. The motion-corrected molecular dimensions are in good agreement with standard values, confirming that

0108-7681/90/040567-06$03.00